

# Electronic structure of titanium oxide clusters: $\text{TiO}_y$ ( $y=1-3$ ) and $(\text{TiO}_2)_n$ ( $n=1-4$ )

Hongbin Wu and Lai-Sheng Wang

Department of Physics, Washington State University, Richland, Washington 99352 and Environmental Molecular Sciences Laboratory, Pacific Northwest National Laboratory, MS K8-88, P.O. Box 999, Richland, Washington 99352

(Received 20 May 1997; accepted 20 August 1997)

The electronic structure of two series of small titanium oxide clusters,  $\text{TiO}_y$  ( $y=1-3$ ) and  $(\text{TiO}_2)_n$  ( $n=1-4$ ), is studied using anion photoelectron spectroscopy. Vibrationally resolved spectra are obtained for  $\text{TiO}^-$  and  $\text{TiO}_2^-$ . Six low-lying electronic states for  $\text{TiO}$  are observed with five of these excited states resulting from multielectron transitions in the photodetachment processes.  $\text{TiO}_2$  is found to be closed-shell with a 2 eV highest occupied molecular orbital/lowest unoccupied molecular orbital (HOMO-LUMO) gap. The two lowest triplet and singlet excited states of  $\text{TiO}_2$  are observed with excitation energies at 1.96 and 2.4 eV, respectively.  $\text{TiO}_3$  is found to have a very high electron affinity (EA) of 4.2 eV, compared to 1.30 and 1.59 eV for  $\text{TiO}$  and  $\text{TiO}_2$ , respectively. The larger  $(\text{TiO}_2)_n$  clusters are all closed-shell with HOMO-LUMO gaps similar to that of  $\text{TiO}_2$  and with increasing EAs: 2.1 eV for  $n=2$ , 2.9 eV for  $n=3$ , 3.3 eV for  $n=4$ . The small HOMO-LUMO gaps for the clusters compared to that of bulk  $\text{TiO}_2$  are discussed in terms of the structure and bonding of these clusters. © 1997 American Institute of Physics. [S0021-9606(97)02444-6]

## I. INTRODUCTION

Titanium dioxide is one of the most technologically important oxide materials and has been widely studied as a prototypical transition metal oxide due to its rather simple electronic structure.<sup>1</sup> Cluster models have been frequently used in theoretical calculations of titanium dioxide bulk or surface properties.<sup>2,3</sup> However, experimental studies on clusters of titanium oxide have been rather scarce. Hagfeldt *et al.* calculated the structure and energy levels of several  $(\text{TiO}_2)_n$  clusters for  $n=1-3$  to understand the chemical and physical properties of bulk  $\text{TiO}_2$ . Experimentally, there are only two previous mass spectrometry studies on the  $\text{Ti}_x\text{O}_y^+$  cluster distributions<sup>6</sup> and no spectroscopic information is known for any  $\text{Ti}_x\text{O}_y$  clusters except  $\text{TiO}$  and  $\text{TiO}_2$ , although there has been considerable interest in the nanoparticles of  $\text{TiO}_2$ .<sup>7</sup>

The  $\text{TiO}$  molecule has been extensively studied spectroscopically because of its astrophysical importance.<sup>8,9</sup> The electronic structure of  $\text{TiO}$  is well understood.<sup>10,11</sup> Considerably less has been reported about the  $\text{TiO}_2$  molecule. There are only two previous calculations<sup>11,12</sup> and three experimental studies,<sup>13-15</sup> which showed that  $\text{TiO}_2$  is a bent molecule and has a singlet ground state.

Our interest is to study the electronic structure and chemical bonding of the small  $\text{Ti}_x\text{O}_y$  clusters using anion photoelectron spectroscopy (PES) which has been shown to be particularly powerful in obtaining electronic structure and spectroscopic information about a wide range of cluster species.<sup>16-21</sup> This information will be valuable to test various theoretical calculations with the intent of understanding bulk properties of  $\text{TiO}_2$ . We are also interested in understanding how the electronic structure of the  $\text{Ti}_x\text{O}_y$  clusters evolves toward that of bulk and discovering unique  $\text{Ti}_x\text{O}_y$  clusters that may be used as reasonable models for bulk surfaces and defect sites.

In the current article, we present a comprehensive study on two series of small titanium oxide clusters,  $\text{TiO}_y$  ( $y=1-3$ ) and  $(\text{TiO}_2)_n$  ( $n=1-4$ ), using the PES technique. In addition to measuring the electron affinity (EA) of these clusters, the PES spectra of the anions also provide information about the low-lying electronic states of the neutral clusters. Vibrationally resolved spectra are obtained for  $\text{TiO}^-$  and  $\text{TiO}_2^-$ . Six low-lying electronic excited states are observed for  $\text{TiO}$  and are assigned using the previous spectroscopic information available for  $\text{TiO}$ . Strong electron correlation effects are observed in  $\text{TiO}$  since five of the observed excited states are due to multielectron detachment transitions.  $\text{TiO}_2$  is found to be a closed shell molecule with a 2 eV highest occupied molecular orbital/lowest unoccupied molecular orbital (HOMO-LUMO) gap. The  $\nu_1$  vibrational frequency of the  $\text{TiO}_2$  ground state is measured to be 960 (40)  $\text{cm}^{-1}$ . The EA of  $\text{TiO}_2$  (1.59 eV) is only slightly higher than that of  $\text{TiO}$  (1.30 eV) while  $\text{TiO}_3$  has a very high EA of about 4.2 eV. The larger  $(\text{TiO}_2)_n$  clusters are all found to be closed shell systems with increasing EA, but the HOMO-LUMO gaps of these larger clusters are about the same as that of the monomer  $\text{TiO}_2$ . This surprising observation of a smaller gap than the bulk rutile  $\text{TiO}_2$  is interpreted on the basis of the structure and bonding of the clusters, which result in a lower coordination for the Ti atoms compared to the bulk.

This article is organized as follows. In Sec. II, the experimental aspects will be briefly described. In Sec. III, we present the experimental results, followed by discussion of the individual clusters in Sec. IV. A brief summary is given in Sec. V.

## II. EXPERIMENT

The experimental apparatus involves a magnetic bottle time-of-flight (TOF) PES analyzer coupled with a laser va-

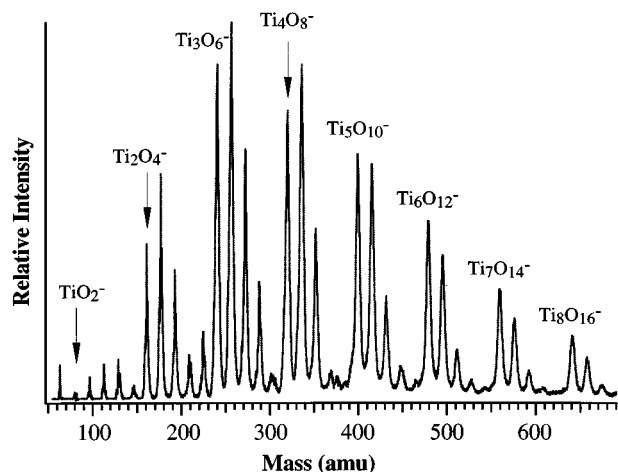


FIG. 1. Negative ion mass spectrum of  $Ti_xO_y^-$  clusters from laser vaporization of a pure Ti target with a helium carrier gas seeded with 5%  $O_2$ .

porization supersonic cluster beam source. The details of the apparatus have been published elsewhere.<sup>16,21</sup> Briefly, a Ti disk target is vaporized by an intense pulsed laser beam from a Nd:YAG laser (10 mJ, 532 nm). The laser-induced plasma is then mixed with a He carrier gas seeded with a small fraction of  $O_2$ . The plasma reactions between the laser-vaporized Ti species and  $O_2$  produce various  $Ti_xO_y$  clusters

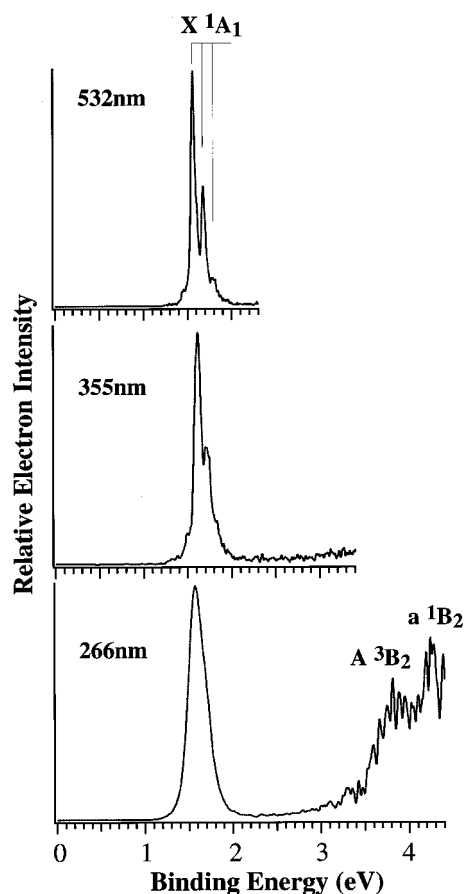


FIG. 3. Photoelectron spectra of  $TiO_2^-$  at 532, 355, and 266 nm.

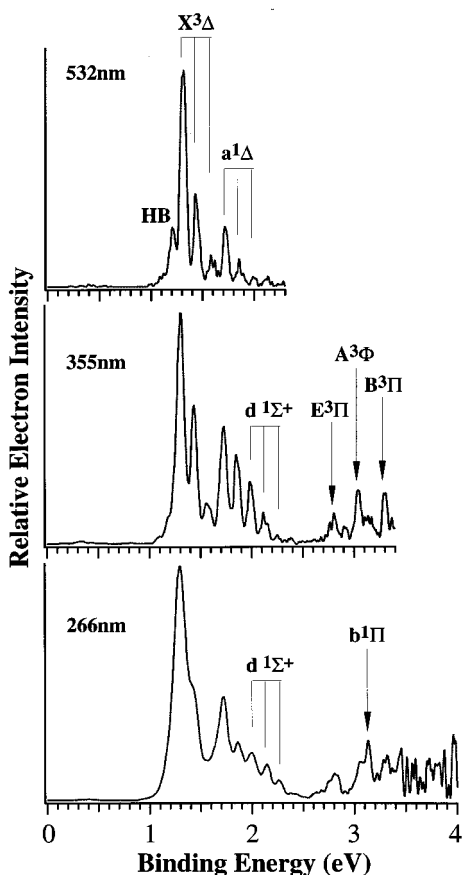


FIG. 2. Photoelectron spectra of  $TiO^-$  at 532, 355, and 266 nm, HB stands for hot band.

in both neutral and charged states. The clusters are expanded into vacuum through a 2-mm-diam nozzle and skimmed to form a collimated cluster beam. The anions in the beam are extracted perpendicularly by a high voltage pulse into a TOF mass spectrometer. The clusters of interest are mass-selected and decelerated before detached by a laser beam from either a Nd:YAG laser (532, 355, 466 nm) or an ArF excimer laser (193 nm). The 532 and 355 nm spectra are taken at 10 Hz repetition rate and the 466 and 193 nm spectra are taken at 20 Hz with the vaporization laser off at alternating shots for background subtraction. The known spectrum of  $Cu^-$  is used for the spectral calibration. The lower detachment photon energies yield higher resolution spectra while the higher photon energies allow more tightly bound electrons to be detached. The latter is especially important for species with high EAs. The spectral resolution is better than 30 meV for 1 eV electrons.

Figure 1 shows a typical anion cluster distribution when a He carrier gas seeded with 5%  $O_2$  is used. Clusters with the  $TiO_2$  stoichiometry and higher O content are produced and are grouped according to the number of Ti atoms. This condition is oxygen-rich and the fully oxidized clusters are produced. When the He carrier gas seeded with 0.5%  $O_2$  is used, partially oxidized clusters with a higher Ti/O ratio are also produced. In this case, a more continuous mass spectrum is

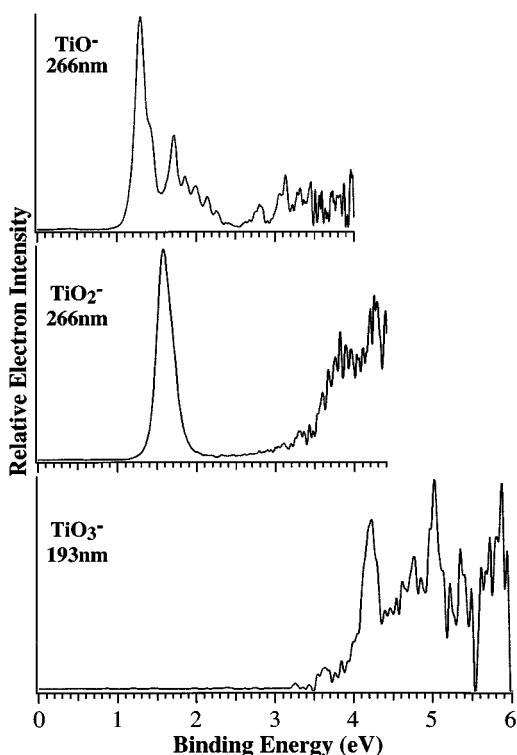


FIG. 4. Photoelectron spectra of  $\text{TiO}_3^-$  at 193 nm compared to the 266 nm spectra of  $\text{TiO}^-$  and  $\text{TiO}_2^-$ .

obtained and overlapping masses with different Ti/O compositions occur due to the mass degeneracy between a Ti atom and three O atoms. In this study, we focus on the  $\text{TiO}_y^-$  ( $y = 1-3$ ) series and the  $(\text{TiO}_2)_n$  series for  $n = 1-4$ . Except for

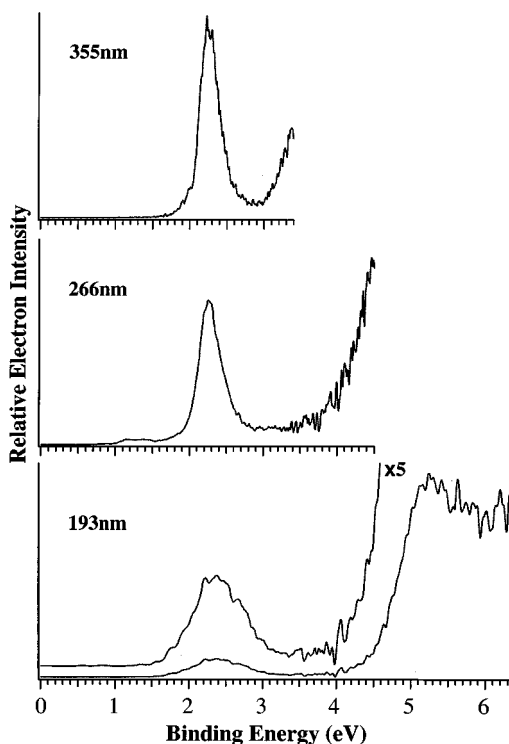


FIG. 5. Photoelectron spectra of  $(\text{TiO}_2)_2^-$  at 355, 266, and 193 nm.

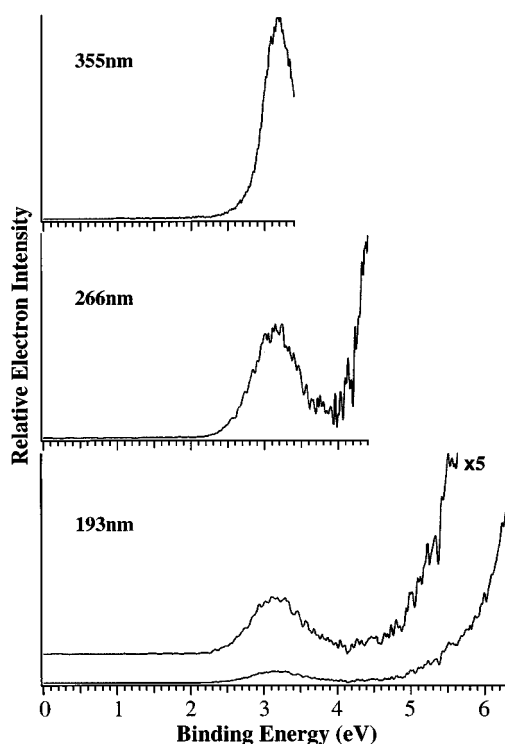


FIG. 6. Photoelectron spectra of  $(\text{TiO}_2)_3^-$  at 355, 266, and 193 nm.

the oxygen-deficient  $\text{TiO}^-$ , which is produced using the 0.5%  $\text{O}_2$  carrier gas, all the other clusters are produced using the oxygen-rich condition of the 5%  $\text{O}_2/\text{He}$  carrier gas.

### III. RESULTS

The PES spectra for the  $\text{TiO}_y^-$  and  $(\text{TiO}_2)_n^-$  species are shown in Figs. 2–8 at various detachment energies ranging from 532 to 193 nm. The spectra of  $\text{TiO}^-$  and  $\text{TiO}_2^-$ , shown in Figs. 2 and 3, respectively, are vibrationally resolved. Six low-lying electronic excited states are observed for  $\text{TiO}$ , as

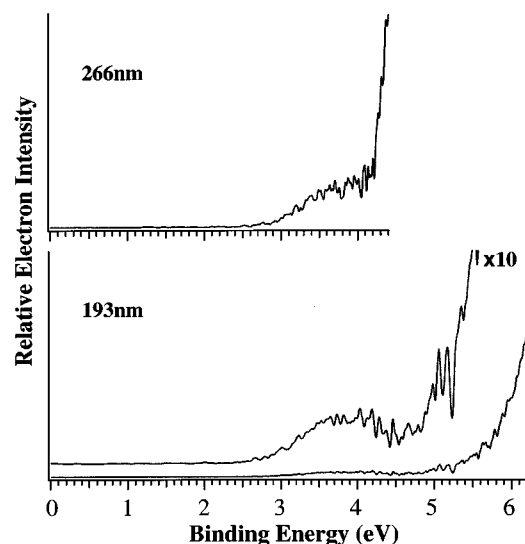


FIG. 7. Photoelectron spectra of  $(\text{TiO}_2)_4^-$  at 266 and 193 nm.

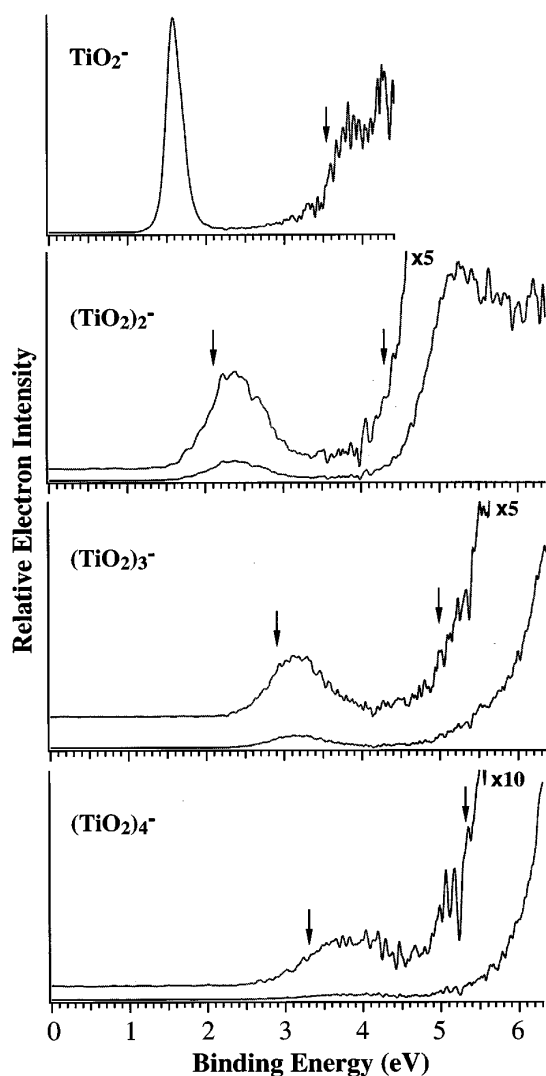


FIG. 8. Comparison of the photoelectron spectra of  $(\text{TiO}_2)_n^-$  for  $n=1-4$ . The arrows indicate the LUMO and HOMO levels.

labeled in Fig. 2. The observed energies and spectroscopic information are listed in Table I for  $\text{TiO}^-$  and  $\text{TiO}$ . For  $\text{TiO}_2^-$ , only one vibrationally resolved band is observed at both 532 and 355 nm. At 266 nm, two more features are observed following a large energy gap of about 2 eV. The

TABLE I. Observed binding energies (BE) and spectroscopic constants for  $\text{TiO}^-$  and  $\text{TiO}$ .

	State	BE (eV)	Term value ( $\text{cm}^{-1}$ ) <sup>a</sup>	Vib. Freq. ( $\text{cm}^{-1}$ ) <sup>a</sup>
$\text{TiO}^-$	$X^1\Sigma^+(9\sigma^1 1\delta^2)$	0	0	800 (60)
$\text{TiO}$	$X^3\Delta(9\sigma^1 1\delta^1)$	1.300 (0.030)	0	1000 (60)
	$a^1\Delta(9\sigma^1 1\delta^1)$	1.725 (0.030)	3430 (60)	1000 (60)
	$d^1\Sigma^+(9\sigma^2)$	2.00 (0.08)	5650 (100)	1000 (80)
	$E^3\Pi(9\sigma^1 4\pi^1)$	2.80 (0.08)	12 100 (100)	
	$A^3\Phi(1\delta^1 4\pi^1)$	3.05 (0.08)	14 110 (100)	
	$b^1\Pi(9\sigma^1 4\pi^1)$	3.13 (0.08)	14 760 (100)	
	$B^3\Pi(1\delta^1 4\pi^1)$	3.31 (0.08)	16 210 (100)	

<sup>a</sup>Relative energies can be determined more accurately.

TABLE II. Observed binding energies (BE) and spectroscopic constants for  $\text{TiO}_2$ .

	BE (eV)	Term value (eV)	Vib. Freq. ( $\text{cm}^{-1}$ )
$X^1A_1$	1.59 (3)		960 (40) <sup>a</sup>
$A^3B_2$	3.55 (10)	1.96 (10)	
$a^1B_2$	4.0 (2) <sup>b</sup>	2.4 (2)	

<sup>a</sup>For the  $\nu_1$  mode.

<sup>b</sup>Estimated.

observed energies and spectroscopic information for  $\text{TiO}_2$  are summarized in Table II. The  $\text{TiO}_3$  species shows a very high EA (Table III) and the spectrum of  $\text{TiO}_3^-$  can only be studied at 193 nm, as shown in Fig. 4 in comparison with that of  $\text{TiO}^-$  and  $\text{TiO}_2^-$ .

The spectra of the larger  $(\text{TiO}_2)_n^-$  clusters are similar to that of  $\text{TiO}_2^-$ , all with a similar energy gap. These suggest that all the stoichiometric  $(\text{TiO}_2)_n$  clusters are closed-shell systems, and the energy gaps represent the HOMO-LUMO gaps of the neutral clusters. However, the EAs of the larger clusters increase with size and the PES spectra of the anions shift to higher binding energy (BE). Thus it becomes difficult to measure the spectra of the large clusters. The EAs of all the clusters are summarized in Table III. The spectra of the large clusters also become broader, due to the fact that the larger clusters are more difficult to cool and the Franck-Condon effect resulting from geometry changes between the ground state of the anions and that of the neutral.

For the 355 nm spectrum of  $(\text{TiO}_2)_2^-$  (Fig. 5), we observe a tail at the high BE side, corresponding to low energy electrons. Compared to the 266 and 193 nm spectra, this tail occurs in the HOMO-LUMO gap region, and is possibly due to either electron scattering (inelastic scattering with chamber walls) or thermionic emissions,<sup>22</sup> both of which are capable of producing low energy electrons. Similar tails are also observed in the 266 nm spectra of  $(\text{TiO}_2)_3^-$  (Fig. 6) and  $(\text{TiO}_2)_4^-$  (Fig. 7). The high noise level at the high BE side is also a factor due to the imperfect background subtraction. The tail in the 266 nm spectrum of  $(\text{TiO}_2)_2^-$  (Fig. 5) signifies the onset of the excited state since it is consistent with the 193 nm spectrum. The weak signals occurring at the lower BE side of the 266 nm spectrum of  $(\text{TiO}_2)_2^-$  is due to a slight contamination of  $\text{Ti}_3\text{O}^-$ , which has the same mass as  $\text{Ti}_2\text{O}_4^-$ . The spectra of all the  $(\text{TiO}_2)_n^-$  ( $n=1-4$ ) series are compared in Fig. 8. The arrows represent the HOMO-LUMO gap in each cluster. Due to the tail of the higher BE feature as shown in Fig. 8, the onset representing the HOMO level in each case can only be estimated. Interestingly, the estimated HOMO-LUMO gaps for all the  $(\text{TiO}_2)_n$  ( $n=1-4$ ) clusters

TABLE III. Measured adiabatic electron affinities (EA) of  $\text{TiO}$ , ( $y=1-3$ ) and  $(\text{TiO}_2)_n$  ( $n=1-4$ ).

	$\text{TiO}$	$\text{TiO}_2$	$\text{TiO}_3$	$\text{Ti}_2\text{O}_4$	$\text{Ti}_3\text{O}_6$	$\text{Ti}_4\text{O}_8$
EA (eV)	1.30 (3)	1.59 (3)	4.2 (1)	2.10 (8)	2.9 (1)	3.3 (2)

are very similar with a value of about 2 eV. Detailed discussion of each cluster follows.

## IV. DISCUSSION

### A. $\text{TiO}^-$

The PES spectra of  $\text{TiO}^-$  are shown in Fig. 2 at three detachment energies. The  $\text{TiO}$  molecule has been well studied and extensively reviewed by Merer in 1989.<sup>8</sup> The electronic structure and many low-lying excited states of  $\text{TiO}$  are known and these make the assignment of the PES spectra shown in Fig. 2 quite straightforward. Six low-lying electronic excited states are observed in the PES spectra and these can all be assigned based on the known energy levels of  $\text{TiO}$ . However, many of these states require multielectron excitations from the photodetachment of  $\text{TiO}^-$ . These multielectron excitations appear to be particularly strong for  $\text{TiO}^-$ , suggesting strong electron correlation effects in this transition metal oxide molecule.

$\text{TiO}$  has a ground state configuration of  $9\sigma^1 1\delta^1 4\pi^0 (X^3\Delta)$ , all the three valence orbitals are primarily of Ti  $3d$  character.<sup>10</sup> In the anion, the extra electron can enter either the  $9\sigma$  or the  $1\delta$  orbital. Since  $\text{TiO}^-$  is isoelectronic with  $\text{VO}$ , which has a  $9\sigma^1 1\delta^2$  configuration,<sup>8</sup> we think that the extra electron in  $\text{TiO}$  enters the  $1\delta$  orbital to give a configuration for  $\text{TiO}^-$  as  $9\sigma^1 1\delta^2 ({}^4\Sigma^-)$ , similar to that of  $\text{VO}$ . The removal of one  $\delta$  electron from  $\text{TiO}^-$  results in the  $X^3\Delta$  ground state of  $\text{TiO}$ , as well as the  $a^1\Delta$  excited state. The 532 nm spectrum in Fig. 2 reveals these two states with vibrational resolution. The spin-orbit splitting for the ground state is too small to be resolved at the current resolution. The observed vibrational frequencies and excitation energy for the  $a^1\Delta$  state are listed in Table I and are in good agreement with the previous optical measurements.<sup>8</sup>

The Franck–Condon factors for the higher vibrational levels of the  $a^1\Delta$  state seem to increase from 532 to 355 nm, as shown in Fig. 2. In particular, the vibrational progression for the  $a^1\Delta$  state becomes rather unusual in the 266 nm spectrum. This suggests that there is another electronic state overlapping with the  $a^1\Delta$  state and whose detachment cross section increases with photon energy. This state actually is the known  $d^1\Sigma^+$  state, whose vibrational frequency is similar to that of the  $a^1\Delta$  state and whose excitation energy overlaps with the  $v=2$  level of the  $a^1\Delta$  state, within our experimental accuracy. The  $d^1\Sigma^+$  state, however, must be due to a two-electron detachment process from the ground state of the anion ( $9\sigma^1 1\delta^2, {}^4\Sigma^-$ ) because it corresponds to a  $9\sigma^2$  configuration.<sup>8</sup> Thus, its weak intensity is understandable.

As shown in the 355 nm spectrum (Fig. 2), at least four more states are observed at BEs of 2.80, 3.05, 3.13, and 3.31 eV. These features all have rather weak intensity and are also observed in the 266 nm spectrum. In particular, the 3.13 eV feature is observed more clearly in the 266 nm spectrum. All of these states can be assigned based on the previous known energy levels of  $\text{TiO}$ , as labeled in Fig. 2 and listed in Table I.<sup>8</sup> However, similar to the  $d^1\Sigma^+$  state, all of these states are due to multielectron transitions in the detachment processes,

consistent with their weak intensity. The  $E^3\Pi$  and  $b^1\Pi$  states are derived from a  $9\sigma^1 4\pi^1$  configuration, due to detachment of a  $1\delta$  electron and promotion of the other  $1\delta$  electron to the  $4\pi$  orbital. Similarly, the  $A^3\Phi$  and  $B^3\Pi$  states are from a  $1\delta^1 4\pi^1$  configuration, due to detachment of a  $1\delta$  electron and promotion of the  $9\sigma$  electron to the  $4\pi$  orbital. Of course, it would be very difficult to assign these states without the knowledge of the energy levels from the previous optical experiments. The excitation energies for these states are all consistent with the known energy levels of  $\text{TiO}$  except that the spin-orbit splittings are not resolved for the  $E^3\Pi$ ,  $A^3\Phi$ , and  $B^3\Pi$  states in the current experiments.

Multielectron excitations are known in photoelectron spectroscopy,<sup>23</sup> which is the major experimental technique to study electron correlation effects in atoms, molecules, and solids. However, observation of such extensive multielectron excitation in the  $\text{TiO}^-$  system is rather unusual. Of course, it is well known that there are strong electron correlation effects in the transition metal systems. Theoretically, systems involving transition metals are very difficult to handle and multireference configuration interaction techniques are required to accurately treat these systems. For the  $\text{TiO}^-$  system, the current experiment suggests that at least configurations involving transfer of electrons among the three  $d$ -type orbitals ( $9\sigma$ ,  $1\delta$ ,  $4\pi$ ) are important to describe the ground state of  $\text{TiO}^-$ .

### B. $\text{TiO}_2^-$

Compared to  $\text{TiO}$ , considerably less has been reported about the  $\text{TiO}_2$  molecule,<sup>11–15</sup> which is known to be a closed shell molecule with a  $C_{2v}$  structure and a bond angle of about  $110^\circ$ . Its vibrational frequencies were measured in a matrix infrared (IR) experiment to be 946.9 and 917.1  $\text{cm}^{-1}$  for the  $\nu_1$  and  $\nu_3$  modes, respectively.<sup>15</sup> An emission band at  $\sim 5300 \text{ \AA}$  (2.34 eV) was observed for  $\text{TiO}_2$  also in a low temperature matrix.<sup>14</sup> Theoretically, Ramana and Philips first treated the ground ( ${}^1A_1$ ) and lowest-lying excited states ( ${}^3B_2$  and  ${}^1B_2$ ) of  $\text{TiO}_2$  in detail using self-consistent-field results (SCF) and configuration interaction (CI) calculations.<sup>12</sup> Their calculations gave an excitation energy of about 1.63 eV for the  ${}^3B_2$  and  ${}^1B_2$  states, which they found were nearly degenerate. Interestingly, their calculations suggested that the  $\text{TiO}_2$  molecule is linear in the excited states.

The PES spectra of  $\text{TiO}_2^-$  are shown in Fig. 3 at three detachment energies. The 532 and 355 nm spectra are very simple, each giving one vibrationally resolved band corresponding to the ground state of  $\text{TiO}_2$ . The observed vibrational mode should be due to the totally symmetric  $\nu_1$  mode. The  $\nu_2$  mode is also allowed, but its frequency, which is not known, is probably too low to be resolved. Our observed frequency for the  $\nu_1$  mode is 940 (40)  $\text{cm}^{-1}$ , in good agreement with the matrix IR experiment mentioned above.<sup>15</sup> The HOMO of  $\text{TiO}_2$  is  $6b_2$ , a weak O–O bonding orbital. The LUMO, where the extra electron enters in  $\text{TiO}_2^-$ , is  $10a_1$ , a nonbonding orbital of Ti  $3d$  character.<sup>12</sup> The removal of the extra electron from the  $10a_1$  orbital of  $\text{TiO}_2^-$  results in the  $X^1A_1$  ground state of  $\text{TiO}_2$ . The vibrational progression of

the ground state suggests that there is only a slight Ti–O bond length change between the anion and the neutral. Therefore, the anion must also have a  $C_{2v}$  structure with a similar bond angle as the neutral  $\text{TiO}_2$ .

Two more features are observed in the 266 nm spectrum at high BE (Fig. 3). The poor signal to noise ratio of these features is due to the low electron energy background presented at this detachment photon energy. These two higher energy features are due to the removal of a  $6b_2$  electron (the HOMO of  $\text{TiO}_2$ ) and are assigned to the  $^3B_2$  and  $^1B_2$  excited states that were studied in the previous theoretical work.<sup>12</sup> The broad nature of the PES spectrum indicates that there must be a large geometry change between the anion and the two  $B_2$  states. The lack of any resolved vibrational structure suggests that the active vibrational mode involved is likely due to the low frequency  $\nu_2$  mode. Therefore, the observed broad detachment features are consistent with the theoretical prediction that the two  $B_2$  states are linear.<sup>12</sup>

The BE of the  $^3B_2$  state is estimated to be 3.55 eV. Due to the overlapping nature between the  $^1B_2$  and the  $^3B_2$  states, the BE for the  $^1B_2$  state is estimated to be at about 4 eV. These yield the excitation energies for the  $^3B_2$  and the  $^1B_2$  to be 1.96 and 2.4 eV, respectively, as given in Table II. The 2.4 eV excitation energy for the  $^1B_2$  state is very close to the 2.34 eV emission spectrum observed for  $\text{TiO}_2$  in the matrix experiment, suggesting that the unassigned emission band is most likely from the  $^1B_2$  excited state to the  $^1A_1$  ground state.<sup>14</sup> Apparently, the previous calculation underestimated the excitation energies for the two  $B_2$  excited states.<sup>12</sup>

### C. $\text{TiO}_3^-$

The spectrum of  $\text{TiO}_3^-$  is shown in Fig. 4, in comparison to those of  $\text{TiO}^-$  and  $\text{TiO}_2^-$ . The  $\text{TiO}_3$  molecule has a very high EA of about 4.2 eV and the spectrum can only be studied at 193 nm. Besides the ground state feature at 4.2 eV, higher energy states are also observed. But due to the poor signal-to-noise statistics, these higher energy features cannot be well identified.

The  $\text{TiO}_3$  molecule has never been studied before either experimentally or theoretically. From  $\text{TiO}$  to  $\text{TiO}_2$ , the formal oxidation state of Ti is increased from +2 to +4, the maximum oxidation state of Ti.  $\text{TiO}_3$  is oxygen-rich because Ti cannot be oxidized to +6. In this case, the  $\text{TiO}_3$  molecule can be viewed to be formed by replacing an O atom in  $\text{TiO}_2$  with an  $\text{O}_2$  peroxide unit. We have observed such oxygen-rich metal oxide molecules with the peroxide unit, for example in  $\text{FeO}_4$ , that also possesses a rather high EA.<sup>20</sup> The bonding between such a peroxide unit and the  $\text{TiO}$  fragment will be interesting to consider theoretically, because the  $\text{O}_2$  peroxide unit is believed to exist on  $\text{TiO}_2$  bulk surfaces.<sup>1</sup> The understanding of this seemingly simple molecular case may help gain insight into the properties of the bulk surfaces.

### D. $(\text{TiO}_2)_n$ , $n=2-4$

There have been very few studies of larger  $\text{TiO}_2$  clusters. Experimentally, there have been two reports on the cation mass distributions of the  $\text{Ti}_x\text{O}_y^+$  clusters<sup>6</sup> and there is no

spectroscopic or structural information on any higher  $\text{Ti}_x\text{O}_y$  clusters other than  $\text{TiO}$  and  $\text{TiO}_2$ . Using a simple pair-potential ionic model, Yu and Freas<sup>6(a)</sup> calculated the minimum energy structures of several  $\text{Ti}_x\text{O}_y$  clusters including the  $(\text{TiO}_2)_n$  clusters for  $n=2-4$ . Hagfeldt *et al.*<sup>4,5</sup> carried out calculations on  $(\text{TiO}_2)_2$  and  $(\text{TiO}_2)_3$ , using *ab initio* SCF methods. They studied both the geometrical and electronic structures of these clusters and were interested in using these clusters as models to understand properties of bulk  $\text{TiO}_2$ . As expected, both of these clusters are closed shell electronic systems with large HOMO-LUMO gaps, which were overestimated in the calculations.  $\text{Ti}_2\text{O}_4$  was shown to have a  $C_{2h}$  structure with a  $\text{Ti}_2\text{O}_2$  rhombus and two terminal O atoms which are bent out of the Ti–Ti axis. The  $\text{Ti}_2\text{O}_4$  structure is very similar to that of  $\text{Si}_2\text{O}_4$  which has a  $D_{2h}$  structure with the two terminal O atoms on the Si–Si axis.<sup>24</sup> The subtle difference between the structures of  $\text{Ti}_2\text{O}_4$  and  $\text{Si}_2\text{O}_4$  reflects the difference in the bonding between Ti and Si with O: *s* and *d* orbitals are involved in Ti while mostly *s* and *p* orbitals are used in Si. The structure of  $\text{Ti}_3\text{O}_6$  found in the previous calculations is also similar to that of  $\text{Si}_3\text{O}_6$  which has a  $D_{2d}$  structure with two perpendicular  $\text{Si}_2\text{O}_2$  rhombuses sharing a central Si atom and two terminal O atoms on the Si–Si–Si axis.<sup>24</sup> The two terminal O atoms in  $\text{Ti}_3\text{O}_6$  are again bent relative to the Ti–Ti–Ti axis, yielding a  $C_s$  structure. For  $\text{Ti}_4\text{O}_8$ , the previous simple pair-potential calculation gave a complicated three-dimensional structure.<sup>6(a)</sup> There is no other more accurate calculation. For the corresponding  $\text{Si}_4\text{O}_8$  cluster, we have previously shown evidence that it may be similar to  $\text{Si}_3\text{O}_6$  with three perpendicular  $\text{Si}_2\text{O}_2$  rhombuses and two terminal O atoms.<sup>26</sup>

Our PES spectra for  $(\text{TiO}_2)_n$  ( $n=2-4$ ) are shown in Figs. 5–7, respectively, at three photon energies: 355, 266, and 193 nm, except  $(\text{TiO}_2)_4^-$  which can only be studied at 266 and 193 nm due to the high EA of neutral  $(\text{TiO}_2)_4$ . All of these clusters show a large HOMO-LUMO energy gap for the neutral clusters, consistent with the previous calculations. However, the calculations overestimated the gaps considerably, probably because relaxation effects were not included.<sup>5</sup> In the anions, the extra electron enters the LUMO of the neutral clusters, producing a doublet ground state for the anions. In the PES spectra shown in Figs. 5–7, the first feature derives from the removal of this extra electron from the LUMO of the neutral clusters, yielding the singlet ground state for the neutrals. The second feature in the spectra shown in Figs. 5–7 corresponds to the removal of an electron from the HOMO of the neutral clusters. Thus the HOMO-LUMO gaps for the neutral clusters are directly measured in the PES spectra. The EAs for the  $(\text{TiO}_2)_n$  clusters, measured from the detachment threshold, are summarized in Table III. They are seen to increase with cluster size, as expected.

Figure 8 compares the spectra for all the  $(\text{TiO}_2)_n^-$  clusters for  $n=1-4$ . The HOMO and LUMO levels are indicated for each cluster. The LUMO level for  $\text{TiO}_2$  is more accurately measured (see Fig. 3) and corresponds to the peak maximum. Two observations are easily made. First, the EAs (LUMO levels) are clearly seen to increase with cluster size. Second, the HOMO-LUMO gaps for all the clusters are seen

to be similar, with a value of about 2 eV. It is particularly surprising that all the larger clusters show similar gaps to that of the  $\text{TiO}_2$  monomer. It is well known that the bulk band gap of the rutile  $\text{TiO}_2$  is 3.1 eV.<sup>27</sup> The question is why the cluster energy gaps are smaller than the bulk value.

There are two possible explanations. First, it is possible that the HOMO levels are underestimated for the  $(\text{TiO}_2)_3$  and  $(\text{TiO}_2)_4$  clusters because of the uncertainty in determining the HOMO levels in the  $(\text{TiO}_2)_3^-$  and  $(\text{TiO}_2)_4^-$  cases as seen in Fig. 8. Second and more plausible, we suspect that the smaller HOMO-LUMO gaps of these small clusters are due to the low coordination number of the Ti atoms compared to that of bulk  $\text{TiO}_2$ . Bulk  $\text{TiO}_2$  crystal has the rutile lattice, where each Ti is coordinated by six O atoms.<sup>1</sup> From our discussions above about the previously calculated structures for  $\text{Ti}_2\text{O}_4$  and  $\text{Ti}_3\text{O}_6$ , they both can be viewed as polymers of the  $\text{TiO}_2$  monomer and the Ti atoms are tetra-coordinated while the terminal Ti atoms are only coordinated to three O atoms with probably a terminal  $\text{Ti}=\text{O}$  double bond. The LUMO levels (corresponding to the conduction band in the bulk) of the clusters should be mainly of Ti 3d character while the HOMO levels (corresponding to the valence band in the bulk) should be mainly of O 2p character. The lower coordination number in the clusters implies a weaker interaction between Ti and O and are probably the cause for the smaller HOMO-LUMO energy splitting. Accordingly, the smaller HOMO-LUMO gap in the  $(\text{TiO}_2)_4$  cluster may suggest that its structure is similar to the  $(\text{TiO}_2)_3$  cluster with three perpendicular  $\text{Ti}_2\text{O}_2$  rhombuses and two terminal O atoms. We stress that this is a tentative observation. More accurate calculations would be desirable in light of the current experiment and should be able to resolve the question regarding the smaller band gaps in these clusters. Direct simulations of the current PES spectra should also allow the structures of these clusters to be definitively determined.<sup>28</sup>

## V. CONCLUSIONS

In conclusion, we have reported the first PES spectra for two series of titanium oxide clusters,  $\text{TiO}_x^-$  ( $x=1-3$ ) and  $(\text{TiO}_2)_n^-$  ( $n=1-4$ ). We have measured the electron affinities of these clusters and presented direct spectroscopic and electronic structure information. For  $\text{TiO}^-$ , the PES spectra reveal distinctly electronic states that result from multielectron transitions. The observation of such intense multielectron processes in the photodetachment of  $\text{TiO}^-$  provides direct experimental evidence for the importance of electron correlation effects and provides quantitative data to test future theoretical calculations. Vibrationally resolved spectra are obtained for the ground state of  $\text{TiO}_2$ . The lowest triplet and singlet excited states of  $\text{TiO}_2$  are measured directly from the PES spectra of  $\text{TiO}_2^-$ . A very high EA for  $\text{TiO}_3$  is measured and it is proposed to contain  $\text{O}_2$  peroxide unit. For the  $(\text{TiO}_2)_n^-$  series, we observe that they are all closed shell systems with a large HOMO-LUMO gap and their EAs increase with size. Surprisingly, the HOMO-LUMO gaps for all the clusters, including the monomer, seem to be similar

( $\sim 2$  eV), which is significantly smaller than the 3.1 eV bulk band gap of rutile  $\text{TiO}_2$ . The smaller gap in the clusters is likely due to the lower coordination number of the Ti atoms, consistent with their proposed structures. The PES spectra of these clusters provide quantitative data which will be valuable to compare to future theoretical calculations to accurately describe the structure and bonding of these clusters.

## ACKNOWLEDGMENTS

This work is supported by The U.S. Department of Energy, Office of Basic Energy Sciences, Chemical Science Division. Pacific Northwest National Laboratory is operated by Battelle for the DOE under Contract No. DE-AC06-76RLO 1830. L.-S. Wang is an Alfred P. Sloan Research Fellow.

- <sup>1</sup> V. E. Henrich and P. A. Cox, *The Surface Science of Metal Oxides* (Cambridge University Press, New York, 1994).
- <sup>2</sup> G. Pachioni, A. M. Ferrari, and P. S. Bagus, *Surf. Sci.* **350**, 159 (1996); C. Sousa and F. Illas, *Phys. Rev. B* **50**, 13 974 (1994).
- <sup>3</sup> A. Hagfeldt, H. O. G. Siegbahn, S.-E. Lindquist, and S. Lunell, *Int. J. Quantum Chem.* **44**, 477 (1992).
- <sup>4</sup> A. Hagfeldt, R. Bergstrom, H. O. G. Siegbahn, and S. Lunell, *J. Phys. Chem.* **97**, 12 725 (1993).
- <sup>5</sup> A. Hagfeldt, S. Lunell, and H. O. G. Siegbahn, *Int. J. Quantum Chem.* **49**, 97 (1994).
- <sup>6</sup> (a) W. Yu and R. B. Freas, *J. Am. Chem. Soc.* **112**, 7126 (1990); (b) B. C. Guo, K. P. Kerns, and A. W. Castleman, *Int. J. Mass Spectrom. Ion Proc.* **117**, 129 (1992).
- <sup>7</sup> M. S. El-Shall, W. Slack, W. Vann, D. Kane, and D. Hanley, *J. Phys. Chem.* **98**, 3067 (1994); J. C. Parker and R. W. Siegel, *J. Mater. Res.* **5**, 1246 (1990); C. A. Melendres, A. Narayanasamy, V. A. Maroni, and R. W. Siedel, *ibid.* **4**, 1246 (1989).
- <sup>8</sup> A. J. Merer, *Ann. Rev. Phys. Chem.* **40**, 407 (1989), and references therein.
- <sup>9</sup> M. Barnes, A. J. Merer, and G. F. Metha, *J. Mol. Spectrosc.* **181**, 180 (1997); L. A. Kaledin, J. E. McCord, and M. C. Heaven, *ibid.* **173**, 499 (1995); A. D. Sappey, G. Eiden, J. E. Harrington, and J. C. Weisshaar, *J. Chem. Phys.* **90**, 1415 (1989); G. M. Daly and M. S. El-Shall, *ibid.* **100**, 1771 (1994).
- <sup>10</sup> E. G. Bakalbassis, M. D. Stiakaki, A. C. Tsipis, and C. A. Tsipis, *Chem. Phys.* **205**, 389 (1996); M. Dolg, U. Wedig, H. Stoll, and H. Preuss, *J. Chem. Phys.* **86**, 2123 (1987); C. W. Bauschlicher, Jr., P. S. Bagus, and C. J. Nelin, *Chem. Phys. Lett.* **101**, 229 (1983).
- <sup>11</sup> R. Bergstrom, S. Lunell, and L. A. Eriksson, *Int. J. Quantum Chem.* **59**, 427 (1996).
- <sup>12</sup> M. V. Ramana and D. H. Phillips, *J. Chem. Phys.* **88**, 2637 (1988).
- <sup>13</sup> M. Kaufman, J. Muentner, and W. Klemperer, *J. Chem. Phys.* **47**, 3365 (1967).
- <sup>14</sup> N. S. McIntyre, K. R. Thompson, and W. Welter, *J. Phys. Chem.* **75**, 3243 (1971).
- <sup>15</sup> G. V. Chertihin and L. Andrews, *J. Phys. Chem.* **99**, 6356 (1995).
- <sup>16</sup> L. S. Wang, H. S. Cheng, and J. Fan, *J. Chem. Phys.* **102**, 9480 (1995).
- <sup>17</sup> H. Wu, S. R. Desai, and L. S. Wang, *J. Chem. Phys.* **103**, 4363 (1995); L. S. Wang, H. Wu, S. R. Desai, and L. Lou, *Phys. Rev. B* **53**, 8028 (1996); H. Wu, S. R. Desai, and L. S. Wang, *J. Phys. Chem.* **101**, 2103 (1997).
- <sup>18</sup> J. Fan and L. S. Wang, *J. Phys. Chem.* **98**, 11 814 (1994); J. Fan, L. Lou, and L. S. Wang, *J. Chem. Phys.* **102**, 2701 (1995); L. S. Wang, *Surf. Rev. Lett.* **3**, 423 (1996).
- <sup>19</sup> H. Wu, S. R. Desai, and L. S. Wang, *Phys. Rev. Lett.* **76**, 212 (1996).
- <sup>20</sup> H. Wu, S. R. Desai, and L. S. Wang, *J. Am. Chem. Soc.* **118**, 5296 (1996); L. S. Wang, H. Wu, and S. R. Desai, *Phys. Rev. Lett.* **76**, 4853 (1996); S. R. Desai, H. Wu, C. Rohlfing, and L. S. Wang, *J. Chem. Phys.* **106**, 1309 (1997).
- <sup>21</sup> L. S. Wang and H. Wu, in *Advances in Metal and Semiconductor Clusters*, edited by M. A. Duncan (JAI, Greenwich, 1997), Vol. IV.
- <sup>22</sup> L. S. Wang, J. Conceicao, C. Jin, and R. E. Smalley, *Chem. Phys. Lett.* **182**, 5 (1991); H. Weideler, D. Kreisle, E. Recknagel, G. Schulze, H.

- Handschuh, G. Gantefor, and W. Eberhardt, *ibid.* **237**, 425 (1995).
- <sup>23</sup>S. Suzer, S. T. Lee, and D. A. Shirley, *Phys. Rev. A* **13**, 1842 (1976).
- <sup>24</sup>L. S. Wang, H. Wu, S. R. Desai, J. Fan, and S. D. Colson, *J. Phys. Chem.* **100**, 8697 (1996).
- <sup>25</sup>L. S. Wang, J. B. Nicholas, M. Dupuis, H. Wu, and S. D. Colson, *Phys. Rev. Lett.* **78**, 4450 (1997).
- <sup>26</sup>L. S. Wang, S. R. Desai, H. Wu, and J. B. Nicholas, *Z. Phys. D* **40**, 36 (1997).
- <sup>27</sup>J. Pascual, J. Camassel, and H. Mathieu, *Phys. Rev. Lett.* **39**, 1490 (1977); *Phys. Rev. B* **18**, 5606 (1978).
- <sup>28</sup>N. Binggeli and J. R. Chelikowsky, *Phys. Rev. Lett.* **75**, 493 (1995); C. Massobrio, A. Pasquarello, and R. Car, *ibid.* **75**, 2104 (1995).